International Journal of Pharmacology and Pharmaceutical Research

ISSN Print: 2664-7184
ISSN Online: 2664-7192
IJPPR 2025; 7(2): 01-07
www.pharmacologyjournals.com
Received: 02-07-2025
Accepted: 04-08-2025

Dheeraj Kumar Vishwakarma
Motherhood University,
Roorkee, Uttarakhand, India

Vaishali Rana
Motherhood University,
Roorkee, Uttarakhand, India

Corresponding Author:
Dheeraj Kumar Vishwakarma
Motherhood University,
Roorkee, Uttarakhand, India

Nrf2/keap1 pathway activation as a mechanism underlying the Renoprotective effects of *Syzygium cumini* in gentamicin-treated wistar rats

Dheeraj Kumar Vishwakarma and Vaishali Rana

DOI: https://www.dx.doi.org/10.33545/26647184.2025.v7.i2a.51

Abstract
Gentamicin, while widely utilized for its efficacy against Gram-negative bacterial infections, is associated with kidney toxicity primarily driven by oxidative damage and inflammatory responses. This study explores the protective influence of *Syzygium cumini* fruit extract on renal injury induced by gentamicin in Wistar rats, particularly emphasizing alterations in the Nrf2/Keap1 signaling pathway. All selected Wistar rats were divided into five (5) groups: a control group, a gentamicin received group, and two (2) treatment groups that received gentamicin combined with (200 mg/kg) and high (400 mg/kg) dose of *S. cumini* and one standard group. Biochemical profiling, tissue analysis, and molecular investigations collectively showed that *S. cumini* significantly improved kidney function and reduced markers of oxidative stress and inflammation. A notable increase in Nrf2 expression along with suppression of Keap1 expression indicated the activation of cellular antioxidant responses. These outcomes indicate the potential of *S. cumini* as a promising plant-based cure for protecting against drug-induced renal damage.

Keywords: Gentamicin, *syzygium cumini*, nephrotoxicity, nrf2/keap1 pathway, oxidative stress etc.

Introduction
Gentamicin, a widely used aminoglycoside antibiotic, is commonly administered for the treatment of E. coli, Klebsiella, Enterobacter spp. infections, but aminoglycosides cause nephrotoxicity in approximately 10-20% of patients [1]. This kidney injury is primarily attributed to oxidative stress, inflammation, and tubular epithelial cell damage [2,3]. The nuclear factor erythroid 2-related factor 2 (Nrf2) act as an indispensable function in cellular defense through regulating the expression of antioxidant enzymes [4]. During oxidative challenges, Nrf2 dissociates from its repressor protein Keap1 (Kelch-like ECH-associated protein 1), enters into the nucleus, and initiates the transcription of genes involved in cytoprotection [5-7]. *Syzygium cumini*, also referred to as jamun, is rich in phytochemicals compounds such as flavonoids, anthocyanins, and ellagic acid, known for their potent antioxidant and anti-inflammatory effects [8-11]. Evidence from animal-based research supports its potential role in managing metabolic disorders and renal impairments [12-14]. The focus of this study is to evaluate the nephroprotective efficacy of *S. cumini* against gentamicin-induced kidney injury in Wistar spp. of (rats), with specific emphasis on its influence over the Nrf2/Keap1 regulatory mechanism.

2. Objectives
- To study the protective potential of *Syzygium cumini* in mitigating gentamicin-induced kidney toxicity.
- To evaluate biochemical markers associated with renal function and oxidative stress.
- To analyze the role of the Nrf2/Keap1 signaling pathway in producing the renoprotective potential of *S. cumini*.

3. Materials and Methods
3.1 Chemicals and Reagents

Table 1: List of Chemicals, Kits, and Reagents Used

S. No.	Material/Reagent	Supplier
1	Gentamicin sulfate	Morksons Pharmaceuticals India Pvt.ltd, Uttarakhand
2	Serum creatinine, BUN, uric acid kits	Shiva Diagnostics
3	RNA extraction kit	Qiagen
4	cDNA synthesis kit	Qiagen
5	Antibodies: Nrf2, Keap1, β-actin	Skymap Pharmaceuticals Pvt Ltd, Roorkee
6	TRIzol reagent	Invitrogen (or specify brand used)
7	Western blotting supplies	Various (e.g., Bio-Rad, Thermo)

3.2 Plant Collection and Extraction

S Ripe fruits of *Syzygium cumini* (L.) were harvested during the fruiting season in April 2025 from local areas around Roorkee district. The plant material was authenticated by a certified scientist of botanist [15]. The collected fruits were thoroughly washed and then left to dry in the shade at ambient laboratory temperature (25-28 °C) for a duration of 10 to 14 days. Once dried, in next steps all dried fruits making into a coarse with help of mechanical grinder. Extraction was performed using 70% ethanol in a Soxhlet apparatus for eight hours. After extraction, the extract was concentrated under low pressure by the rotary evaporator at a temperature range of 40-45°C, yielding a semisolid ethanolic extract. This extract was subsequently transferred to an amber-colored bottle and final extract stored at 4°C for further experimental procedure [16,17].

3.3 Experimental Animals and Grouping

After animals were acclimated for one week, twenty-five experimental animals (Wistar rats), having a weight between 180 and 220 grams. The animals were housed in polypropylene cages under standard laboratory conditions, kept under a 12:12-hour light-dark cycle, with standard pellet diet and clean drinking.

A total of 30 experimental rats were randomly distributed into five groups, with six rats per group (n = 6):

Table 2: Groups of animals.

Group	Treatment	Number of rats
I	Normal control (saline)	06
II	Gentamicin -80 mg/kg I.P. for each day, (7 days)	06
III	Gentamicin + *S. cumini* extract (200 mg/kg/day orally)	06
IV	Gentamicin + *S. cumini* extract (400 mg/kg/day orally)	06
V	Gentamicin + Cystone (400 mg/kg/day orally)	06

3.4 Assessment of Renal Function

At the completion of the study period, blood samples were removed from the retro-orbital plexus under light anaesthetic condition. The obtained blood was centrifuged to separate the serum, which was then analyzed for the following biochemical parameters:

Biochemical Estimation Procedures

Serum Creatinine Estimation [18]

Serum creatinine was measured using the Jaffe reaction, under alkaline conditions, creatinine undergoes a reaction with picric acid forming a red-orange chromophore. Following the manufacturer's instructions, serum samples were mixed with the provided reagent and incubated for the specified duration. The absorbance was then measured spectrophotometrically within the 520-540 nm range. Creatinine concentration level was quantified by comparing the sample absorbance to that of a known calibration curve.

Blood Urea Nitrogen (BUN) Estimation [19]

Blood urea nitrogen (BUN) levels were estimated using an enzyme-catalyzed colorimetric technique based on urease activity. Urease catalyzes the breakdown of urea into ammonia, it subsequently interacts with phenol and hypochlorite, in the presence of sodium nitroprusside, yielding a blue-green chromophore. Serum samples were first incubated with a urease-containing reagent, subsequently added by the addition of color-developing agents. After incubation, reading of absorbance taken at 570 nm with spectrophotometer. BUN concentrations were determined with help known calibration curve.

Uric Acid Estimation [20]

Serum uric acid was measured using the uricase-peroxidase enzymatic method. Uric acid + O_2 + H_2O → Allantoin + CO_2 + H_2O_2. The H_2O_2 produced then reacts with peroxidase and, forming a colored compound. The sample of serum were incubated at 37°C with the reagent containing uricase and chromogen. Absorbance was recorded between 520 and 550 nm using a spectrophotometer. Uric acid concentration was measured via a standard curve.

Total Protein Estimation [21]

Total protein levels were estimated by Biuret method; samples were mixed with reagent and stand at 25 degrees siliceous for 10 to 15 minutes. Absorbance was then measured at 540-560 nm using a spectrophotometer, with a reagent blank as reference. Protein concentration was measured via a standard curve.

Proteins + Cu^{2+} (in alkaline medium) → Violet-colored Cu-protein complex

Albumin Estimation [22]

Serum albumin was estimated by the BCG dye-binding method. The assay involved adding the BCG reagent to the serum sample, then incubate at room temperature for 1 to 5 minutes. Absorbance was recorded between 620 and 640 nm using a spectrophotometer.

Albumin + Bromocresol Green (BCG) → Green-colored Albumin-BCG Complex (in acidic medium)

Serum Sodium (Na^+) Estimation [23]

Serum sodium concentration was measured using either the flame photometry method or the ion-selective electrode (ISE) technique. In flame photometry, the serum sample was

aspirated into a flame, and the intensity of the yellow light emitted by sodium ions (Na^+) was detected. Sodium levels were calculated by comparing the emission intensity to that of standard sodium solutions.

Serum Chloride (Cl^-) Estimation [24]
Serum chloride levels were determined using a colorimetric method involving mercuric thiocyanate. In this reaction, chloride ions displace thiocyanate, which then reacts with ferric ions to produce a red-colored complex. Ferric nitrate and mercuric thiocyanate were added to serum samples, and absorbance was measured between 480 and 520 nm with help of spectrophotometer. Chloride concentration was calculated by comparation of the absorbance.

Serum Potassium (K^+) Estimation [25]
Serum potassium concentration was measured using either flame photometry or the ion-selective electrode (ISE) method. In the flame photometric technique, diluted serum samples were aspirated into a flame, and the emission at 766.5 nm characteristic of potassium ions (K^+) was recorded. Potassium levels were quantified by comparing the emission intensity with that of standard potassium solutions.

Aspartate Aminotransferase (AST) Estimation [26]
Aspartate aminotransferase (AST) catalyzes the following reaction:
L-Aspartate + α-Ketoglutarate ⟶ Oxaloacetate + L-Glutamate
The oxaloacetate formed reacts with 2,4-dinitrophenylhydrazine (DNPH) to form a colored hydrazone complex: Oxaloacetate + DNPH ⟶ Oxaloacetate-DNPH Hydrazone (colored complex)
Upon addition of sodium hydroxide (NaOH), the color intensifies, and the absorbance of the complex is measured at 505 nm by spectrophotometer.

Alanine Aminotransferase (ALT) Estimation [27]
Alanine aminotransferase (ALT) catalyzes the transamination of alanine and α-ketoglutarate, resulting in the formation of pyruvic acid ($C_3H_4O_3$) and glutamate ($C_5H_9NO_4$). Pyruvic acid reacted with 2,4-dinitrophenylhydrazine (DNPH) to form a carbonyl complex. After the addition of sodium hydroxide (NaOH), a colored product developed, and its absorbance was taken at 505 nm using a spectrophotometer. ALT activity was determined by comparing the absorbance with that of a standard reference.

Alkaline Phosphatase (ALP) Estimation [28]
p-Nitrophenyl phosphate (pNPP) + H_2O ⟶ p-Nitrophenol (pNP) + Phosphate (PO_4^{3-})
Under alkaline pH, p-nitrophenol exists in its yellow-colored anionic form, which absorbs strongly at 405 nm.

Lactate Dehydrogenase (LDH) Estimation [29]
Lactate dehydrogenase (LDH) activity was measured based on its catalytic role in the Lactate + NAD^+ ⇌ Pyruvate + NADH + H^+, accompanied by the reduction of NAD^+ to NADH. The activity was quantified by monitoring the reduce in absorbance at 340 nm, equivalent to the oxidation of NADH to NAD^+.

Creatine Kinase (CK) Estimation [30]
Creatine Phosphate + ADP ⇌ Creatine + ATP. The ATP generated was utilized in a coupled enzymatic reaction that produced NADPH, which was quantified by taking the increase in absorbance at 340 nm.

Malondialdehyde (MDA) Estimation [31]
Malondialdehyde (MDA) + 2 Thiobarbituric Acid (TBA) ⟶ $MDA\text{-}TBA_2$ Adduct (Pink-colored complex). This adduct has a peak absorbance at 532 nm, which can be measured spectrophotometrically.

Reduced Glutathione (GSH) Estimation [32]
The level of reduced glutathione was determined using the reagent 5,5'-dithiobis-(2-nitrobenzoic acid) which forms a yellow compound with GSH which absorbs maximally at 412 nm. The proteins were precipitated with TCA (trichloroacetic acid) with some vigor, and the resulting clear supernatant was collected into sterile tubes. The supernatant was mixed with DTNB and the absorbance of the reaction product measured at 412 nm with a spectrophotometer to determine the GSH concentration.

Superoxide Dismutase (SOD) Activity [33]
Superoxide dismutase (SOD) activity was measured as its ability to inhibit the auto-oxidation of epinephrine in alkaline conditions. The rise in absorbance caused by the reaction was monitored at 480 nm with a spectrophotometer. One unit of SOD activity was defined as the amount of enzyme that inhibited 50% of epinephrine auto-oxidation.

Catalase (CAT) Activity [34]
The catalase activity was assessed based on the decomposition of hydrogen peroxide (H_2O_2) into water and oxygen. A tissue homogenate sample was placed into a reaction mixture containing hydrogen peroxide. Absorbance at 240 nm was monitored using a spectrophotometer, and the reduction in absorbance was noted. Catalase catalyzed the breakdown of hydrogen peroxide, and the reduction of absorbance showed this reaction took place.

Neutrophil Gelatinase-Associated Lipocalin (NGAL) Estimation [35]
An early indicator of acute kidney injury, Neutrophil gelatinase-associated lipocalin (NGAL), was assessed with a commercial ELISA kit following the provided protocols. Serum samples were placed into microplate wells coated with NGAL-specific antibodies. After the incubation stage, color development was achieved with TMB. Its intensity was read at 450 nm on a spectrophotometer.

Kidney Injury Molecule-1 (KIM-1) Estimation [36]
Kidney Injury Molecule-1 (KIM-1) concentrations were measured using a sandwich ELISA method. Serum and urine samples were added to microtiter plate wells which were coated with KIM-1 specific capture antibodies. After washing, enzyme-linked detection antibodies were added which formed an antigen-antibody complex. A color development reaction using the appropriate substrate was performed and absorbance was measured at 450nm. The formed optical density was proportional to the KIM-1 concentration in tested samples.

Interleukin-6 (IL-6) Estimation [38]
The levels of Interleukin-6 (IL-6) were quantified using a sandwich ELISA with capture and detection monoclonal antibodies. Following sample incubation and washing with

wells coated with capture antibodies, color development was initiated with the addition of substrate solution. IL-6 concentration was determined by measuring the absorbance at 450 nm with a microplate reader and comparing with a standard curve.

C-Reactive Protein (CRP) Estimation [39]

An acute-phase inflammatory marker, C-reactive protein (CRP), was measured by means of an immunoturbidimetric assay. Mixing serum samples with anti-CRP antibodies yielded CRP immunoturbidometric complexes and CRP antibodies, which formed turbidity. CRP concentration was measured by comparing with a standard curve after the absorbance at the 570 nm was read spectrophotometrically

Histopathological Examination [40]

Kidney tissues were preserved in 10% neutral buffered formalin, dehydrated, and embedded in paraffin wax. The tissues were sliced into sections of 5 µm which were mounted on glass slides. The mounted sections were stained with H and E and analyzed with light microscope to assess any morphological changes.

Molecular Analysis (RT-PCR & Western Blot)

RNA isolation: Total RNA extraction was conducted using TRIzol reagent on the kidney tissues obtained. As outlined in the protocol, kidney tissue samples underwent homogenization in TRIzol, followed by chloroform treatment for phase separation. The RNA was collected from the aqueous phase, precipitated with isopropanol, and then washed with 75% ethanol. The RNA was air-dried and then resuspended in RNase-free water. The integrity, concentration, and purity of the RNA was assessed using a spectrophotometer [41].

RT-PCR: Complementary DNA (cDNA) was synthesized from 1 µg of total RNA using a commercial reverse transcription kit, as per the manufacturer's protocol. PCR amplification was carried out using gene-specific primers targeting Nrf2, Keap1, and β-actin (used as an internal control). The resulting PCR products were separated by agarose gel electrophoresis and visualized under ultraviolet (UV) illumination [42].

Western blotting: Kidney tissues were homogenized in RIPA buffer supplemented with protease and phosphatase inhibitors to prevent protein degradation. Protein concentrations were determined using the Bradford assay. Equal amounts of protein from each sample were separated by SDS-PAGE and transferred onto PVDF membranes. The membranes were blocked with 5% non-fat dry milk to prevent non-specific binding, followed by incubation with primary antibodies specific for Nrf2 and Keap1. After washing, membranes were incubated with HRP-conjugated secondary antibodies. Protein bands were visualized using enhanced chemiluminescence (ECL) reagents, and band intensities were quantified using dedicated image analysis software [43].

3.8. Statistical Analysis

Results are reported as the mean ± standard deviation (S.D.). One-way ANOVA was utilized to assess differences between groups. If variance was significantly different as determined by ANOVA, means comparison on a priori defined groups was made using Tukey's post hoc test. A value of $p<0.05$ was accepted as statistically significant.

4. Results and Discussion

4.1 Renal Function Tests

Gentamicin administration significantly increased serum levels of creatinine, blood urea nitrogen (BUN), and uric acid, indicating the onset of nephrotoxicity. However, treatment with *Syzygium cumini* extract especially at the 400 mg/kg dose effectively mitigated these elevations, restoring the biochemical parameters closer to normal values.

Table 3: Determination of BUN, Creatinine and Uric acid.

Group	Creatinine (mg/dL)	BUN (mg/dL)	Uric Acid (mg/dL)
Control	0.7±0.03	18.1±1.1	2.4±0.3
Gentamicin(100/kg)	2.4±0.14**	55.5±2.6**	6.0±0.4**
SC-L (200 mg/kg)	1.4±0.09*	35.6±1.8*	4.0±0.3*
SC-H (400 mg/kg)	0.9±0.06*	22.1±1.3*	2.7±0.2*
Standard (Cystone-400 mg/kg)	0.6± 0.03	19.6±0.1	2.6±2.2

Notes: Values are expressed as Mean±SEM (n = X; insert sample size). *$p<0.05$ vs. Gentamicin group (significant)., **$p<0.01$ vs. Control group (gentamicin-induced elevation).

Table 4: Effect of Treatments on Serum Protein and Electrolytes

Group	Total Protein (g/dL)	Albumin(g/dL)	Sodium(mEq/L)	Chloride(mEq/L)	Potassium(mEq/L)
Control	6.8±0.3	3.7±0.1	142.6±2.0	102.2±1.8	4.2±0.3
Gentamicin (100mg/kg)	4.9±0.3 **	2.4±0.1 **	128.3±2.5 **	71.5±2.2 **	6.1±0.4 **
SC-L (200 mg/kg)	5.9±0.2 *	3.2±0.2 *	133.7±1.9 *	88.6±1.7 *	5.1±0.3 *
SC-H (400 mg/kg)	6.5±0.2 *	3.5±0.1 *	138.8±2.0 *	98.3±1.4 *	4.5±0.2 *
Standard (Cystone-400 mg/kg)	6.6± 0.3	3.6±0.1	139.6±2.2	100.2±1.8	4.1±0.3

Notes: Values are expressed as Mean ± SEM (n = X; insert sample size). *$p<0.05$ vs. Gentamicin group (significant)., **$p<0.01$ vs. Control group (gentamicin-induced elevation).

Table 5: Effect of Treatments on Liver Enzymes and Cellular Injury Markers

Group	AST (U/L)	ALT (U/L)	ALP (U/L)	LDH (U/L)	CK (U/L)
Control	47.2±3.5	36.5±2.1	112.4±6.3	146.7±7.8	132.1±5.6
Gentamicin(100mg/kg)	95.3±4.8 **	78.6±3.9 **	224.5±9.2 **	280.3±10.4 **	265.2±8.7 **
SC-L (200 mg/kg)	68.9±3.2 *	54.2±2.5 *	158.3±6.7 *	198.7±9.1 *	185.4±6.3 *
SC-H (400 mg/kg)	51.7±2.9 *	40.1±2.2 *	124.9±5.5 *	162.5±8.4 *	147.3±5.1 *
Standard (Cystone-400 mg/kg)	48.6± 3.3	38.6±2.1	119.6±5.2	140.2±4.8	140.2±4.8

Notes: Values are expressed as Mean ± SEM (n = X; insert sample size). *$p<0.05$ vs. Gentamicin group (significant)., **$p<0.01$ vs. Control group (gentamicin-induced elevation).

Table 6: Effect of Treatments on Oxidative Stress, Renal Injury, and Inflammatory Markers

Parameter	Control	Gentamicin (100mg/kg)	SC-L (200 mg/kg)	SC-H (400 mg/kg)	Standard (Cystone-400 mg/kg)
MDA(nmol/mg protein)	1.7±0.2	4.9±0.4 **	3.1±0.3 *	2.1±0.2 *	1.6±0.3
GSH (µmol/mg protein)	5.6±0.4	2.1±0.3 **	3.8±0.3 *	4.8±0.4 *	5.3±0.1
SOD (U/mg protein)	12.4±1.1	5.1±0.6 **	8.7±0.8 *	11.1±0.9 *	10.4±1.3
CAT (U/mg protein)	46.3±2.5	21.8±1.9 **	33.2±2.1 *	41.6±2.7 *	45.3±2.5
NGAL (ng/mL)	45.2±3.2	123.4±6.5 **	84.7±4.8 *	58.2±3.9 *	44.2±4.2
KIM-1 (ng/mL)	62.5±4.1	138.7±7.3 **	95.6±5.1 *	71.2±4.4 *	60.1±4.2
TNF-α (pg/mL)	28.3±2.7	64.5±4.2 **	42.8±3.6 *	33.6±2.9 *	27.1±1.7
IL-6 (pg/mL)	36.4±3.1	82.3±5.1 **	56.9±3.9 *	41.3±3.2 *	34.8±2.1
CRP (mg/L)	1.5±0.2	5.7±0.4 **	3.1±0.3 *	2.1±0.2 *	1.4±0.3

Notes: Values are expressed as Mean ± SEM (n = X; insert sample size). *p<0.05 vs. Gentamicin group (significant)., **p<0.01 vs. Control group (gentamicin-induced elevation).

4.2 Nrf2/Keap1 Expression

Expression Analysis of Nrf2 and Keap1 by RT-PCR and Western Blot: The mRNA and protein expression levels of Nrf2 and Keap1 were assessed across different treatment groups using RT-PCR and Western blot densitometry. As shown in Table 6, gentamicin administration (100 mg/kg) led to a significant downregulation of Nrf2 expression and a corresponding upregulation of Keap1, both at the transcriptional and protein levels, when compared to the control group. Treatment with *Syzygium cumini* extract at low (200 mg/kg) and high doses (400 mg/kg) significantly reversed these changes. The high-dose group (SC-H) showed marked enhancement in Nrf2 mRNA and protein expression and a substantial reduction in Keap1 levels, indicating a dose-dependent activation of the antioxidant defense pathway. The standard drug group (Cystone, 400 mg/kg) also demonstrated a similar trend of gene and protein modulation. These findings suggest that *S. cumini* confers renal protection by regulating the Nrf2/Keap1 signaling axis, consistent with previous reports on herbal antioxidants modulating oxidative stress markers (Jung *et al*., 2016; Kansal *et al*., 2020).

Table 7: Expression of Nrf2 and Keap1 at mRNA and Protein Levels in Different Treatment Groups

Gene/Protein	Control	Gentamicin (100 mg/kg)	SC-L (200 mg/kg)	SC-H (400 mg/kg)	Standard (Cystone 400 mg/kg)
Nrf2 (RT-PCR fold change)	1.00±0.05	0.42±0.04**	0.73±0.06*	0.95±0.05	0.91±0.04
Keap1 (RT-PCR fold change)	1.00±0.07	1.81±0.09**	1.32±0.08*	1.08±0.06	1.11±0.07
Nrf2 (Western blot densitometry)	1.00±0.06	0.46±0.05**	0.77±0.07*	0.98±0.06	0.93±0.05
Keap1 (Western blot densitometry)	1.00±0.04	1.76±0.08**	1.35±0.06*	1.07±0.05	1.09±0.04

Values are expressed as mean±SD (n = 6).

*Significant compared to gentamicin group (p<0.05); **Highly significant compared to control group (p<0.01); Comparable to control (p>0.05).

4.3 Histopathology

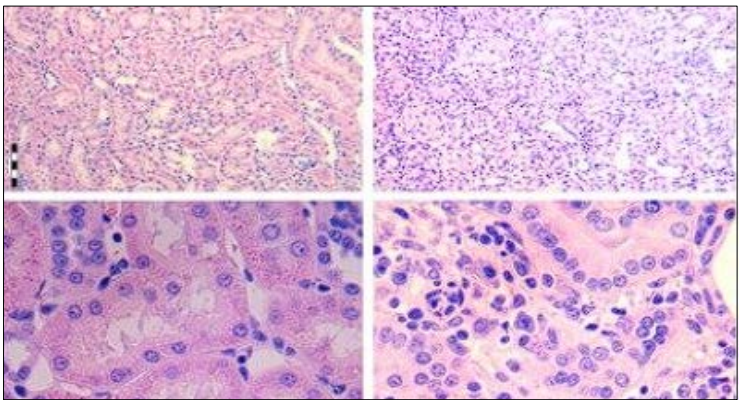

Fig 1: Histopathological sections of renal tissue

In the control group, kidney tissue showed normal structure with clearly visible tubules and glomeruli. Gentamicin-treated animals exhibited noticeable kidney damage, including glomerular congestion, tubular cell death, and formation of casts. Mild structural changes such as limited tubular damage and reduced inflammation were observed in rats given a low dose of *Syzygium cumini* extract (SC-L). Those treated with a high dose (SC-H) had kidneys that appeared largely normal, with only slight alterations, indicating strong protective effects against gentamicin-induced kidney injury.

Conclusion

The findings of this study suggest that *Syzygium cumini* provides protective effects against gentamicin-induced kidney damage, primarily through activation of the Nrf2/Keap1 antioxidant signaling pathway. Its bioactive components may serve as a potential phytotherapeutic

option for managing acute kidney injury linked to oxidative stress. Further studies are needed to isolate specific compounds and explore their clinical applications.

References

1. Ali BH, Al Za'abi M, Blunden G, Nemmar A. Experimental gentamicin nephrotoxicity and agents that modify it: a mini-review of recent research. Basic Clin Pharmacol Toxicol. 2011;109(4):225-232.
2. Walker PD, Shah SV. Gentamicin enhanced production of hydrogen peroxide by renal cortical mitochondria. Am J Physiol. 1987;253(3):F452-F455.
3. Balakumar P, Rohilla A, Thangathirupathi A. Gentamicin-induced nephrotoxicity: do we have a promising therapeutic approach to blunt it? Pharmacol Res. 2010;62(3):179-186.
4. Kaspar JW, Niture SK, Jaiswal AK. Nrf2:INrf2 (Keap1) signaling in oxidative stress. Free Radic Biol Med. 2009;47(9):1304-1309.
5. Ma Q. Role of nrf2 in oxidative stress and toxicity. Annu Rev Pharmacol Toxicol. 2013;53:401-426.
6. Kensler TW, Wakabayashi N, Biswal S. Cell survival responses to environmental stresses via the Keap1-Nrf2-ARE pathway. Annu Rev Pharmacol Toxicol. 2007;47:89-116.
7. Tonelli C, Chio II, Tuveson DA. Transcriptional regulation by Nrf2. Antioxid Redox Signal. 2018;29(17):1727-1745.
8. Sharma B, Balomajumder C, Roy P. Hypoglycemic and hypolipidemic effects of *Syzygium cumini* in alloxan-induced diabetic rats. Food Chem Toxicol. 2008;46(7):2376-2383.
9. Bhowmik D, Yadav A, Tripathi K, Kumar K. Traditional medicinal plants with antioxidant activity. J Med Plants Stud. 2012;1(1):56-61.
10. Sagrawat H, Khan A, Kumar A. Phytochemical evaluation and hepatoprotective activity of ethanolic extract of *Syzygium cumini* bark. Pharmacogn Mag. 2006;2(6):96-100.
11. Bhattacharya S. Reactive oxygen species and cellular defense system. Free Radicals Antioxid. 2015;5(2):13-19.
12. Halliwell B, Gutteridge JM. Free radicals in biology and medicine. 5th ed. Oxford: Oxford University Press; 2015.
13. Valko M, Rhodes CJ, Moncol J, Izakovic M, Mazur M. Free radicals, metals and antioxidants in oxidative stress-induced cancer. Chem Biol Interact. 2006;160(1):1-40.
14. Liu M, Grigoryev DN, Crow MT, Haas M, Yamamoto M, Reddy SP. Transcription factor Nrf2 is protective during ischemic and nephrotoxic acute kidney injury in mice. Kidney Int. 2009;76(3):277-285.
15. Warrier PK, Nambiar VPK, Ramankutty C. Indian medicinal plants: a compendium of 500 species. Vol. 5. Hyderabad: Orient Blackswan; 1996. p. 245-247.
16. Harborne JB. Phytochemical methods: a guide to modern techniques of plant analysis. London: Springer; 1998.
17. Khandelwal KR. Practical pharmacognosy: techniques and experiments. 23rd ed. Pune: Nirali Prakashan; 2019. p. 149-152.
18. Fabiny DL, Ertingshausen G. Automated reaction-rate method for determination of serum creatinine with the CentrifiChem. Clin Chem. 1971;17(8):696-700.
19. Fawcett JK, Scott JE. A rapid and precise method for the determination of urea. J Clin Pathol. 1960;13(2):156-159.
20. Caraway WT. Uric acid. In: Seligson D, editor. Standard methods of clinical chemistry. New York: Academic Press; 1963. p. 239-247.
21. Gornall AG, Bardawill CJ, David MM. Determination of serum proteins by means of the biuret reaction. J Biol Chem. 1949;177(2):751-766.
22. Doumas BT, Watson WA, Biggs HG. Albumin standards and the measurement of serum albumin with bromocresol green. Clin Chim Acta. 1971;31(1):87-96.
23. Varley H, Gowenlock AH, Bell M. Practical clinical biochemistry. 5th ed. London: Heinemann; 1980.
24. Tietz NW. Fundamentals of clinical chemistry. 3rd ed. Philadelphia: WB Saunders; 1987.
25. Zall DM, Fisher DF, Garner MD. Photometric determination of chloride in biological fluids. Anal Chem. 1956;28(11):1665-1668.
26. Reitman S, Frankel S. A colorimetric method for the determination of serum glutamic oxaloacetic and glutamic pyruvic transaminases. Am J Clin Pathol. 1957;28(1):56-63.
27. Reitman S, Frankel S. A colorimetric method for the determination of serum glutamic pyruvic transaminase. Am J Clin Pathol. 1957;28(1):56-63.
28. Kind PRN, King EJ. Estimation of plasma phosphatase by determination of hydrolysed phenol with antipyrine. J Clin Pathol. 1954;7(4):322-326.
29. Wroblewski F, LaDue JS. Lactic dehydrogenase activity in blood. Proc Soc Exp Biol Med. 1955;90(1):210-213.
30. Oliver IT. A spectrophotometric method for the determination of creatine phosphokinase and myokinase. Biochem J. 1955;61(1):116-122.
31. Ohkawa H, Ohishi N, Yagi K. Assay for lipid peroxides in animal tissues by thiobarbituric acid reaction. Anal Biochem. 1979;95(2):351-358.
32. Ellman GL. Tissue sulfhydryl groups. Arch Biochem Biophys. 1959;82(1):70-77.
33. Misra HP, Fridovich I. The role of superoxide anion in the autoxidation of epinephrine and a simple assay for superoxide dismutase. J Biol Chem. 1972;247(10):3170-3175.
34. Aebi H. Catalase *in vitro*. Methods Enzymol. 1984;105:121-126.
35. Mishra J, Ma Q, Prada A, Mitsnefes M, Zahedi K, Yang J, *et al*. Identification of neutrophil gelatinase-associated lipocalin as a novel early urinary biomarker for ischemic renal injury. J Am Soc Nephrol. 2003;14(10):2534-2543.
36. Han WK, Bailly V, Abichandani R, Thadhani R, Bonventre JV. Kidney injury molecule-1: a tissue and urinary biomarker for nephrotoxicant-induced renal injury. Am J Physiol Renal Physiol. 2002;283(4):F867-F874.
37. Bradley PP, Priebat DA, Christensen RD, Rothstein G. Measurement of cutaneous inflammation: estimation of neutrophil content with an enzyme marker. J Invest Dermatol. 1982;78(3):206-209.
38. Dinarello CA. Interleukin-6 and the pathogenesis of inflammatory diseases. N Engl J Med. 2000;342(20):1516-1527.

39. Tillett WS, Francis T Jr. Serological reactions in pneumonia with a non-protein somatic fraction of pneumococcus. J Exp Med. 1930;52(4):561-571.
40. Bancroft JD, Gamble M. Theory and practice of histological techniques. 6th ed. Philadelphia: Churchill Livingstone Elsevier; 2008. p. 83-134.
41. Chomczynski P, Sacchi N. Single-step method of RNA isolation by acid guanidinium thiocyanate-phenol-chloroform extraction. Anal Biochem. 1987;162(1):156-159.
42. Bustin SA, Nolan T. Pitfalls of quantitative real-time reverse-transcription polymerase chain reaction. J Biomol Tech. 2004;15(3):155-166.
43. Towbin H, Staehelin T, Gordon J. Electrophoretic transfer of proteins from polyacrylamide gels to nitrocellulose sheets: procedure and some applications. Proc Natl Acad Sci USA. 1979;76(9):4350-4354.
44. Burnette WN. “Western blotting”: electrophoretic transfer of proteins from sodium dodecyl sulfate-polyacrylamide gels to unmodified nitrocellulose and radiographic detection with antibody and radioiodinated protein A. Anal Biochem. 1981;112(2):195-203.